Journal of Statistical Physics, Vol. 125, No. 3, November 2006 (© 2006)
DOI: 10.1007/s10955-006-9051-9

Quadrupolar Ordering of Phospholipid Molecules in Narrow Necks of Phospholipid Vesicles

Veronika Kralj-Iglič,[1,2] Blaž Babnik,[2] Dorit R. Gauger,[3] Sylvio May,[3,4] and Aleš Iglič[2]

Received September 10, 2004; accepted July 19, 2005
Published Online: October 4, 2006

Shapes of phospholipid vesicles that involve narrow neck(s) were studied theoretically. It is taken into account that phospholipid molecules are intrinsically anisotropic with respect to the membrane normal and that they exhibit quadrupolar orientational ordering according to the difference between the local principal membrane curvatures. Direct interactions between oriented molecules were considered within a linear approximation of the energy coupling with the deviatoric field. The equilibrium shapes of axisymmetric closed vesicles were studied by minimization of the free energy of the phospholipid bilayer membrane under relevant geometrical constraints. The variational problem was stated by a system of Euler-Lagrange differential equations that revealed a singularity in the derivative of the meridian curvature at points where the effect of the orientational ordering exactly counterbalances the effect of the isotropic bending. The system of Euler-Lagrange differential equations was solved numerically to yield consistently related equilibrium orientational distribution of the phospholipid molecules and vesicle shape. According to our estimation of the model constants the formation of the neck is promoted if direct interactions between the oriented molecules are taken into account. It was shown that the energy of the equilibrium shapes is considerably affected by the quadrupolar ordering of phospholipid molecules.

KEY WORDS: phospholipid vesicle shape, neck, deviatoric bending, curvature singularity, quadrupolar ordering

[1] Institute of Biophysics, Faculty of Medicine, University of Ljubljana, Lipičeva 2, SI-1000 Ljubljana, Slovenia
[2] Laboratory of Physics, Faculty of Electrical Engineering, University of Ljubljana, Tržaška 25, SI-1000 Ljubljana, Slovenia
[3] Research group "Lipid Membranes," Friedrich-Schiller University, Neugasse 25, Jena 07745, Germany
[4] Present address: North Dakota State University, Department of Physics, Box 5566, Fargo, ND 58105-5566, U.S.A

1. INTRODUCTION

Phospholipid bilayers that form the basis of cellular membranes are the subject of extensive studies, as they exhibit a large variety of interesting physical phenomena regarding the configuration of the phospholipid molecules, as well as regarding the macroscopically observable shapes of vesicular structures. In the last 30 years most attention was devoted to shapes where the principal curvature radii of the membrane are much larger than the dimensions of the membrane[1] so that the membrane could be treated as an almost flat, elastic, laterally isotropic, two dimensional continuum.[2,3,4] Minimization of the energy of isotropic bending[2,3] by solving a system of Euler differential equations[5] yielded a phase diagram of possible equilibrium shapes. To assess the relevant energy of these shapes it is now acknowledged that the area–difference–elasticity model (ADE model)[8,9] provides an explanation of many interesting features in bilayer membrane systems[4),(9–12].

More recently, it became evident that the phospholipid membrane also forms nanostructures such as long thin tubes attached to almost flat parts of the membrane,[13–18] while indirect evidence on membrane permeability indicates that pores are formed within cellular membranes.[19–20] At least one of the principal curvature radii of the membrane is small in nanotubular protrusions and in pores (of the order of tens of nanometers in the case of nanotubes and of the order of the membrane layer thickness in the case of membrane pores). Further, within these nanostructures the two local principal curvatures are considerably different.

Experiments with erythrocytes have shown that the erythrocyte membrane undergoes budding after addition of amphiphilic substances to the erythrocyte suspension, as the amphiphilic molecules intercalate into the phospholipid bilayer. For certain amphiphilic substances, micro and nanostructures with regions of considerably different principal curvatures were observed. These structures include tubular buds and vesicles,[21] nonspherical micro and nanovesicles,[21] torocyte endovesicles[22,23] and thin tubular connections between the membrane compartments.[14] It was found that addition of octaethyleneglycol (C12E8) to the erythrocyte suspension induces formation of torocytic endovesicles[22] - thin flat structures with a toroid-like end and that the same substance stabilizes membrane pores induced by electroporation in the DC3F cell line.[24]

Recently, a theoretical description was put forward providing a possible explanation for the stability of all the above described membrane shapes with connected nanostructures.[18),(25–27] The proposed theory is based on the notion that a membrane constituent is characterized by its intrinsic shape - i.e. the shape of the surrounding continuum that would require no energy to accommodate the constituent. However, due to constraints within the many-constituent system, such a situation is not possible for all the constituents. The energy cost of inserting a phospholipid molecule into the membrane at a particular site reflects the mismatch between the intrinsic shape given by the intrinsic principal curvatures and the ac-

tual shape given by the local principal curvatures. The two intrinsic principal curvatures are in general different which allows for quadrupolar ordering of the membrane constituents according to the local difference between the two principal curvatures[28,25] Derivation of the free energy of the phospholipid membrane by the methods of statistical physics[18] yields the expression for the energy of local isotropic bending[3] while it also yields a new term of negative sign that contributes at regions where the two principal curvatures are different.[18] Quadrupolar ordering of the constituents in the deviatoric field at such regions thus lowers the free energy of the system.

Notable changes in collective ordering of phospholipid molecules within bilayers are exhibited by phase transitions[29,30] and reflected in the vesicle shape. It was shown[31] that a collective tilt of phospholipid molecules promotes a saddle shape of the membrane. The existence of a phase transition indicates the existence of direct interactions between the phospholipid molecules which are therefore also present above the phase transition temperature causing a weaker, yet possibly significant effect (similar to the interaction of magnetic moments with an external magnetic field and with other magnetic moments that are above the phase transition temperature, exhibited in the susceptibility of the system).

It has also been observed[32] that the main phase transition is sensitive to the curvature of the membrane layer which therefore acts as an effective external field. These data support our assumption that ordering of the molecules may be different in different parts of the membrane, depending on the local curvature of the membrane.

As well as in previously studied systems that involve nanotubular protrusions, torocytes and pores, a high difference between the principal membrane curvatures could also be attained in a stable narrow neck that is eventually formed in the process of budding.

Stability of a narrow neck was observed, for example, in spontaneous shape transformation of a POPC (palmitoyl-oleoyl-phosphatidylcholine) vesicle obtained by electroformation where the undulated tubular protrusion slowly shortened and integrated into the globular mother vesicle.[25] If a small void was left in the observation chamber that allowed for slight evaporation of water, the beads that formed the protrusion became sphere-like while the necks became very thin so that they could not be observed by the phase contrast microscope. In this case the sequence leading to a globular vesicle did not evolve and the observed shape with "spherical" beads stayed stable for hours.[25] The possibility should be considered that the necks that connect the vesicular compartments are very thin, of the order of tens of nanometers, and that a mechanism similar to that explaining the stability of connected nanotubes and pores is also important in necks.

In this work we apply the above mentioned theoretical description that provides an explanation for the observed membrane shapes with connected nanostructures (where the two principal curvatures strongly differ) to the shapes

of phospholipid vesicles with neck(s). We study the sequence where with increasing average mean curvature of the vesicle the prolate vesicle shape transforms into a shape composed of two spheres connected by a narrow neck whose width decreases in the process. The membrane free energy for a one-component phospholipid membrane was derived previously.[18] Here we introduce some modifications in the description. We introduce a two-state model of the orientational ordering so as to obtain simple analytical expressions in the formulation of the variational problem. The variational problem for axisymmetric vesicle shapes can then be expressed by a system of Euler-Lagrange differential equations[5] and solved numerically to yield an equilibrium shape and an orientational distribution of the constituents that are consistently related. The consistently related effects of the orientational ordering and the vesicle shape are to our knowledge rigorously considered for the first time. Within the applied approach, direct interactions between the oriented molecules are taken into account. The expression of the variational problem and the obtained solutions may add to the understanding of the stability of narrow necks of phospholipid membranes and support the hypothesis of quadrupolar ordering of the membrane constituents as a possible mechanism that is important in phospholipid bilayer systems.

2. THEORY

2.1. The Two State Model

A single phospholipid molecule is treated as a point-like constituent in a two-dimensional continuum curvature field imposed by the other phospholipid molecules. We assume that the phospholipid molecule, due to its structure and local interactions, energetically would prefer a local geometry that is described by the two principal curvatures $C_{1\mathrm{m}}$ and $C_{2\mathrm{m}}$. As the phospholipid molecule is composed of two tails and a headgroup, the intrinsic principal curvatures are in general not identical i.e. the intrinsic shape of the phospholipid molecule is anisotropic.[18] If the area and the volume of the vesicle are fixed, the shape cannot attain the curvatures that would equal the intrinsic curvatures in all its points and the energy of the molecules is increased. The energy of a single molecule derives from the mismatch between the actual membrane shape given by the two principal curvatures C_1 and C_2 and the intrinsic shape given by the intrinsic principal curvatures $C_{1\mathrm{m}}$ and $C_{2\mathrm{m}}$,[25,28]

$$E(\omega) = \frac{\xi}{2}(H - H_{\mathrm{m}})^2 + \frac{\xi + \xi^*}{4}\left(\hat{C}^2 - 2\hat{C}\hat{C}_{\mathrm{m}}\cos(2\omega) + \hat{C}_{\mathrm{m}}^2\right), \qquad (1)$$

where ξ and ξ^* are constants describing the strength of the interaction between the molecule and the surrounding membrane, $H = (C_1 + C_2)/2$ is the mean curvature of the membrane, $H_{\mathrm{m}} = (C_{1\mathrm{m}} + C_{2\mathrm{m}})/2$ is the mean curvature of the continuum

intrinsic to the molecule, $\hat{C} = (C_1 - C_2)/2$, $\hat{C}_m = (C_{1m} - C_{2m})/2$ and ω is the orientation of the principal axes of the intrinsic shape relative to the principal axes of the local curvature of the continuum.

It can be seen from (1) that the single-molecule energy attains a minimum when $\cos(2\omega) = 1$, *i.e.* when the two systems are aligned or mutually rotated by an angle π, while the single-molecule energy attains a maximum when $\cos(2\omega) = -1$, *i.e.* when the two systems are mutually rotated by an angle $\pi/2$ or $3\pi/2$. In the first case the single-molecule energy is

$$E_{\min} = \frac{\xi}{2}(H - H_m)^2 + \frac{\xi + \xi^*}{4}\left(D^2 + D_m^2\right) - \frac{\xi + \xi^*}{2} D D_m, \tag{2}$$

whereas in the second case the single-molecule energy is

$$E_{\max} = \frac{\xi}{2}(H - H_m)^2 + \frac{\xi + \xi^*}{4}\left(D^2 + D_m^2\right) + \frac{\xi + \xi^*}{2} D D_m, \tag{3}$$

where $D = \mid \hat{C} \mid$ and $D_m = \mid \hat{C}_m \mid$ are the curvature deviator and the intrinsic curvature deviator, respectively. The states $\omega = 0, \pi$ and $\omega = \pi/2, 3\pi/2$, respectively, are degenerate. We say that the ordering is quadrupolar.

2.2. Local Equilibrium of Independent Molecules

Each monolayer is described separately. The contributions to the free energy of the two monolayers are then summed to obtain the energy of the bilayer membrane.

The monolayer area is divided into small patches which however contain a large number of molecules so that methods of statistical physics can be used. The membrane curvature is taken to be constant over the patch. We consider that all phospholipid molecules are equal and independent and are subject to the curvature field. The lattice statistics approach is used, drawing an analogy from the problem of noninteracting magnetic dipoles in an external magnetic field,[33] the curvature deviator D taking the role of the external magnetic field.

In the idealized case, we assume a simple model where we have M equivalent molecules in the patch, each of which can exist in one of two possible states corresponding to the energies $E_{\min}$ and $E_{\max}$, respectively (Eqs. (2) and (3)); N molecules are taken to be in the state with higher energy $E_{\max}$ and $(M - N)$ molecules are taken to be in the state with lower energy $E_{\min}$. The energy of the lipid molecules within the patch in the mean curvature field, divided by kT where k is the Boltzmann constant and T is the temperature, is

$$\frac{E_D}{kT} = N\frac{E_{\max}}{kT} + (M - N)\frac{E_{\min}}{kT} \quad . \tag{4}$$

Inserting Eqs. (2) and (3) into Eq. (4) gives

$$\frac{E_D}{kT} = M\frac{E_q}{kT} - (M/2 - N)d_{\text{eff}}, \tag{5}$$

where

$$\frac{E_q}{kT} = \frac{\xi}{2kT}(H - H_m)^2 + \frac{\xi + \xi^*}{4kT}\left(D^2 + D_m^2\right), \tag{6}$$

and

$$d_{\text{eff}} = \frac{(\xi + \xi^*)D_m D}{kT}. \tag{7}$$

We call d_{eff} the effective curvature deviator.

Direct interactions between the molecules are taken into account. The curvature field that is considered in this description is produced by the molecules themselves, i.e. the molecules pack together in such way as to form the local shape of the membrane. Therefore, the orientation of a given molecule is important regarding the interaction with its nearest neighbors. In describing the direct interaction between the nearest neighbor molecules, we propose it should be taken into account that the molecules which are oriented in such way that their orientational energy in the mean curvature field is lower, also exhibit more favorable packing. By attaining the shape that is in tune with the local curvature field, the tails of the favorably oriented molecules come on the whole closer together, which gives rise to additional lowering of the energy of the patch due to direct interactions, relative to the situation where the molecules are randomly oriented within the patch. On the other hand, if we consider that the molecules which are oriented in such way that their orientational energy in the mean curvature field is higher, exhibit less favorable packing in which the tails are on the whole further apart. This causes a rise of the energy of the interaction between such oriented molecules within the patch with respect to the situation where the molecules are randomly oriented. The effect depends on the local curvature field, on the intrinsic shape of the molecule and the strength of the interaction. We take it that the effect is proportional to the local effective curvature deviator. The direct interaction of N molecules in the patch that have higher energy $E_{\max}$, with their neighbors is therefore described by a positive contribution,

$$\frac{E_N}{kT} = \frac{\tilde{k}}{kT}Nd_{\text{eff}}, \tag{8}$$

where $\tilde{k}$ is the interaction constant. Accordingly, the direct interaction of $(M - N)$ molecules that have lower energy $E_{\min}$, with their neighbors is described as

$$\frac{E_{M-N}}{kT} = -\frac{\tilde{k}}{kT}(M - N)d_{\text{eff}}. \tag{9}$$

The total energy of the patch due to direct interaction E_{i}/kT is $(E_N/kT + E_{M-N}/kT)/2$, where we divide by 2 as to avoid counting each molecule twice. Therefore,

$$\frac{E_{\mathrm{i}}}{kT} = -\frac{\tilde{k}}{kT}(M/2 - N)d_{\mathrm{eff}}. \tag{10}$$

The total energy of the patch E^{P} is obtained by summing the contribution of the orientation of the molecules according to the local curvature deviator E_D and the contribution of the direct interaction between the molecules within the patch E_{i},

$$\frac{E^{\mathrm{p}}}{kT} = \frac{E_D}{kT} + \frac{E_{\mathrm{i}}}{kT}. \tag{11}$$

The chosen patch is considered as a system with a constant area A^{p} and a constant number of molecules M. The system is immersed in a heat bath so that its temperature T is constant. There are two possible energy states for the molecules in the patch. Within the given energy state the molecules are treated as indistinguishable. We assume that the system is in thermodynamic equilibrium and follow the description of a two-orientation model of noninteracting magnetic dipoles.[33] Analogous, if there are N molecules in the state with higher (maximal) energy and $(M - N)$ molecules in the state with lower (minimal) energy, the number of possible arrangements consistent with this N is $M!/N!(M - N)!$, while the corresponding energy of the system is E^{P}. However, when calculating the partition function, we must consider all possibilities, e.g., N can be any number from 0 to M; $N = 0$ means that all the molecules are in the state with lower energy, $N = 1$ means that one molecule is in the state with higher energy while $M - 1$ molecules are in the state with lower energy, etc.. The canonical partition function $Q^{\mathrm{p}}(M, T, D)$ of M molecules in the small patch of the membrane is therefore

$$Q^{\mathrm{p}} = \sum_{N=0}^{M} \frac{M!}{N!(M-N)!} \exp\left(-\frac{E^{\mathrm{P}}}{kT}\right), \tag{12}$$

where k the Boltzmann constant.

Considering Eqs. (2)–(12) yields

$$Q^{\mathrm{P}} = q^M \sum_{N=0}^{M} \frac{M!}{N!(M-N)!} \exp\left(d_{\mathrm{eff}}(1 + \tilde{k}/kT)(M/2 - N)\right), \tag{13}$$

where by considering Eq. (6)

$$q = \exp\left(-\frac{E_{\mathrm{q}}}{kT}\right). \tag{14}$$

Using the binomial (Newton) formula in summation of the finite series in Eq. (13) gives

$$Q^{\mathrm{P}} = (2q\cosh(d_{\mathrm{eff}}(1+\tilde{k}/kT)/2))^{M}. \tag{15}$$

The Helmholtz free energy of the patch is $F^{\mathrm{P}} = -kT\ln Q^{\mathrm{P}}$,

$$F^{P} = \frac{M(3\xi+\xi^{*})}{4}H^{2} - M\xi H H_{m} - \frac{M(\xi+\xi^{*})}{4}C_{1}C_{2} - MkT\ln\left(2\cosh\left(\frac{d_{\mathrm{eff}}(1+\frac{\bar{k}}{kT})}{2}\right)\right) + \frac{M\xi}{2}H_{m}^{2} + \frac{M(\xi+\xi^{*})}{4}D_{m}^{2} \tag{16}$$

where we used the relation

$$D^{2} = H^{2} - C_{1}C_{2}. \tag{17}$$

The energy of the membrane bilayer is then obtained by summing the contributions of the all patches in both monolayers,

$$F = \int_{A_{\mathrm{out}}} m_{\mathrm{out}}F^{\mathrm{P}}(C_{1},C_{2})\,\mathrm{d}A + \int_{A_{\mathrm{in}}} m_{\mathrm{in}}F^{\mathrm{P}}(-C_{1},-C_{2})\,\mathrm{d}A, \tag{18}$$

where m_{out} and m_{in} are the area densities of the lipid molecules in the outer and in the inner monolayer, respectively, while F^{P} is given by Eq. (16). It is considered that the signs of the principal curvatures in the inner layer are opposite to the signs of the principal curvatures in the outer layer.

We assume that $m_{\mathrm{out}} = m_{\mathrm{in}} = m_{0}$. Also, in integration, we neglect the difference between the areas of the two monolayers ($A_{\mathrm{out}} = A_{\mathrm{in}} = A$), where A is the membrane area. The latter approximation is not valid for strongly curved membranes, but in the system that will be considered in this work, the area corresponding to strong curvature (i.e. the area of the neck(s)) is small compared to the area of the entire vesicle. It follows from Eqs. (16) and (18) that

$$F = \frac{(3\xi+\xi^{*})}{8}m_{0}\int(2H)^{2}\mathrm{d}A - \frac{(\xi+\xi^{*})m_{0}}{2}\int C_{1}C_{2}\mathrm{d}A - 2m_{0}kT\int\ln(2\cosh(d_{\mathrm{eff}}(1+\tilde{k}/kT)/2))\mathrm{d}A, \tag{19}$$

where the constant terms are omitted. The first two terms of the above expression yield the bending energy of a nearly flat thin membrane.[3] In the following, the constant contribution $-2m_{0}kT\,A\ln 2$ that is included in the third term of Eq. (19) is omitted. Also the second term in Eq. (19) is not considered further since according to the Gauss-Bonnet theorem it is constant for the closed surfaces that are considered in this work. Therefore we will further consider the expression for

the free energy F,

$$F = \frac{(3\xi + \xi^*)}{8} m_0 \int (2H)^2 \mathrm{d}A - 2m_0 kT \int \ln\cosh(d_{\mathrm{eff}}(1 + \tilde{k}/kT)/2)\mathrm{d}A. \quad (20)$$

2.3. The Degree of Ordering of Phospholipid Molecules

The average number of molecules in each of the energy states represents the local quadrupolar ordering of the molecules. Knowing the canonical partition function of a patch Q^{P} we can calculate the average number of molecules with higher energy within the patch ($E_{\max}$),

$$\langle N \rangle = \frac{\sum_{N=0}^{M} N \frac{M!}{N!(M-N)!} \mathrm{e}^{-d_{\mathrm{eff}}(1+\tilde{k}/kT)N}}{\sum_{N=0}^{M} \frac{M!}{N!(M-N)!} \mathrm{e}^{-d_{\mathrm{eff}}(1+\tilde{k}/kT)N}}, \quad (21)$$

while the average number of the molecules with lower energy within the patch ($E_{\min}$) is

$$\langle M - N \rangle = \frac{\sum_{N=0}^{M} (M-N) \frac{M!}{N!(M-N)!} \mathrm{e}^{-d_{\mathrm{eff}}(1+\tilde{k}/kT)N}}{\sum_{N=0}^{M} \frac{M!}{N!(M-N)!} \mathrm{e}^{-d_{\mathrm{eff}}(1+\tilde{k}/kT)N}}, \quad (22)$$

Equation (21) can be rewritten in the form

$$\langle N \rangle = -\frac{\partial \ln Q_0^{\mathrm{P}}}{\partial(d_{\mathrm{eff}}(1 + \tilde{k}/kT))}, \quad (23)$$

where

$$Q_0^{\mathrm{P}} = \sum_{N=0}^{M} \frac{M!}{N!(M-N)!} \mathrm{e}^{-d_{\mathrm{eff}}(1+\tilde{k}/kT)N} = \left(1 + \mathrm{e}^{-d_{\mathrm{eff}}(1+\tilde{k}/kT)}\right)^M. \quad (24)$$

It follows from Eqs. (23) and (24) that the average fraction of the molecules in the higher energy state $E_{\max}$ can be expressed as

$$\frac{\langle N \rangle}{M} = \frac{1}{1 + \mathrm{e}^{d_{\mathrm{eff}}(1+\tilde{k}/kT)}}, \quad (25)$$

while the average fraction of the molecules in the lower energy state $E_{\min}$ is

$$\frac{\langle M - N \rangle}{M} = \frac{1}{1 + e^{-d_{\mathrm{eff}}(1+\tilde{k}/kT)}}. \quad (26)$$

It can be seen from Eqs. (25)–(26) that at $d_{\mathrm{eff}} = 0$, i.e. when the principal curvatures are equal, both energy states are equally occupied ($\langle N \rangle / M = \langle M - N \rangle / M = 1/2$). The fraction of the number of molecules in the lower energy state increases with increasing d_{eff} to 1, while the fraction of molecules in the higher energy state decreases to 0.

2.4. Global Thermodynamic Equilibrium

The equilibrium configuration of the system (the equilibrium shape and the corresponding distribution of the quadrupolar ordering) is sought by minimizing the membrane free energy

$$\delta F = 0 \tag{27}$$

under relevant geometrical constraints. We require that the membrane area A be fixed

$$\int \mathrm{d}A = A, \tag{28}$$

that the enclosed volume V be fixed

$$\int \mathrm{d}V = V \tag{29}$$

and that the average mean curvature $\langle H \rangle$

$$\langle H \rangle = \frac{1}{A} \int H \mathrm{d}A \tag{30}$$

be fixed.

For clarity, the above problem is expressed in dimensionless form. We introduce the dimensionless curvatures $c_1 = R_\mathrm{s} C_1$, $c_2 = R_\mathrm{s} C_2$, $h = R_\mathrm{s} H$, $h_\mathrm{m} = R_\mathrm{s} H_\mathrm{m}$, $\langle h \rangle = R_\mathrm{s} \langle H \rangle$, $d = R_\mathrm{s} D$, $d_\mathrm{m} = R_\mathrm{s} D_\mathrm{m}$, the relative area $a = A/4\pi {R_\mathrm{s}}^2 = 1$, the relative volume $v = 3V/4\pi {R_s}^3$, the relative area element $\mathrm{d}a = \mathrm{d}A/4\pi R_\mathrm{s}^2$ and the relative volume element $\mathrm{d}v = 3\mathrm{d}V/4\pi R_\mathrm{s}^3$. The normalization unit R_s is the radius of the sphere of the required area A, $R_s = \sqrt{A/4\pi}$. The free energy of the phospholipid bilayer F (Eq. (20)) is normalized relative to $(3\xi + \xi^*)2\pi m_0$,

$$f = w_\mathrm{b} + f_\mathrm{d}, \tag{31}$$

where

$$w_\mathrm{b} = \frac{1}{4} \int (c_1 + c_2)^2 \mathrm{d}a, \tag{32}$$

$$f_\mathrm{d} = -\kappa \int \ln \cosh(d_\mathrm{eff}(1 + \tilde{k}/kT)/2) \mathrm{d}a \tag{33}$$

and

$$\kappa = 4kT {R_s}^2 / (3\xi + \xi^*). \tag{34}$$

We consider only axisymmetric shapes. The geometry of the shape is described in terms of the arc length l. We use the coordinates $\rho(l)$ and $z(l)$ where ρ is the perpendicular distance between the symmetry axis and a certain point on the

contour and z is the position of this point along the symmetry axis. The principal curvatures are

$$c_1 = \frac{\sin\psi}{\rho}, c_2 = \frac{\mathrm{d}\psi}{\mathrm{d}l} \equiv \psi_l, \tag{35}$$

where ψ is the angle between the normal to the surface and the symmetry axis. The dimensionless area element is $\mathrm{d}a = \rho \mathrm{d}l/2$ and the dimensionless volume element is $\mathrm{d}v = 3\rho^2 \sin\psi \mathrm{d}l/4$. Using the above coordinates, the dimensionless free energy is

$$f = \int \frac{1}{8}\left(\frac{\sin\psi}{\varrho} + \psi_l\right)^2 \rho \mathrm{d}l - \int \frac{\kappa\rho}{2} \ln\cosh\left(\vartheta\left(\frac{\sin\psi}{\varrho} - \psi_l\right)\right)\mathrm{d}l. \tag{36}$$

where

$$\vartheta = \frac{(\xi + \xi^*)D_\mathrm{m}}{4kTR_s}\left(1 + \frac{\tilde{k}}{kT}\right) \quad , \tag{37}$$

while the dimensionless global constraints are

$$\int \frac{1}{2}\rho \mathrm{d}l = 1, \tag{38}$$

$$\int \frac{3}{4}\rho^2 \sin\psi \mathrm{d}l = v \tag{39}$$

and

$$\int \frac{1}{4}(\sin\psi + \psi_l\rho)\mathrm{d}l = \langle h\rangle. \tag{40}$$

Also, we must consider a local constraint between the chosen coordinates,

$$\frac{\mathrm{d}\rho}{\mathrm{d}l} = \cos\psi. \tag{41}$$

A functional is constructed,

$$G = \int \mathcal{L}\mathrm{d}l \quad , \tag{42}$$

where

$$\mathcal{L} = \frac{1}{8}\left(\frac{\sin\psi}{\varrho} + \psi_l\right)^2 \rho - \frac{\kappa\rho}{2}\ln\cosh\left(\vartheta\left(\frac{\sin\psi}{\varrho} - \psi_l\right)\right)$$
$$+ \lambda_a\frac{\rho}{2} + \lambda_v\frac{3}{4}\rho^2\sin\psi + \lambda_{\langle h\rangle}\frac{1}{4}\left(\frac{\sin\psi}{\varrho} + \psi_l\right)\rho + \lambda(\rho_l - \cos\psi), \tag{43}$$

λ_a, λ_v and λ_h are the global Lagrange multipliers and λ is the local Lagrange multiplier. The above variational problem is expressed by a system of Lagrange-Euler differential equations,

$$\frac{\partial \mathcal{L}}{\partial \rho} - \frac{\mathrm{d}}{\mathrm{d}l}\left(\frac{\partial \mathcal{L}}{\partial \rho_l}\right) = 0, \tag{44}$$

$$\frac{\partial \mathcal{L}}{\partial \psi} - \frac{\mathrm{d}}{\mathrm{d}l}\left(\frac{\partial \mathcal{L}}{\partial \psi_l}\right) = 0. \tag{45}$$

It follows from Eqs. (44) and (43) that

$$\frac{\mathrm{d}\lambda}{\mathrm{d}l} = \frac{1}{8}\left(\frac{\chi^2 - \sin^2\psi}{\rho^2}\right) + \frac{\lambda_a}{2} + \frac{3}{2}\lambda_v \varrho \sin\psi + \frac{1}{4}\lambda_{\langle h\rangle}\frac{\chi}{\rho} - \frac{\kappa}{2}\ln\cosh\left(\vartheta\left(\frac{\sin\psi - \chi}{\varrho}\right)\right) + \frac{\kappa\vartheta}{2\rho}\sin\psi\tanh\left(\vartheta\left(\frac{\sin\psi - \chi}{\varrho}\right)\right), \tag{46}$$

while it follows from Eqs. (45) and (43) that

$$\frac{\mathrm{d}\chi}{\mathrm{d}l} = \frac{\mathcal{A}}{\mathcal{B}} \tag{47}$$

where

$$\mathcal{B} = \left(1 - \frac{2\kappa\vartheta^2}{\cosh^2\left(\vartheta\left(\frac{\sin\psi-\chi}{\varrho}\right)\right)}\right), \tag{48}$$

$$\mathcal{A} = \frac{\sin\psi\cos\psi}{\rho}\left(1 + \frac{2\kappa\vartheta^2}{\cosh^2\left(\vartheta\left(\frac{\sin\psi-\chi}{\varrho}\right)\right)}\right) - \frac{4\kappa\vartheta^2\chi\cos\psi}{\rho\cosh^2\left(\vartheta\left(\frac{\sin\psi-\chi}{\varrho}\right)\right)} + 3\lambda_v\varrho^2\cos\psi + 4\lambda\sin\psi - 4\kappa\vartheta\cos\psi\tanh\left(\vartheta\left(\frac{\sin\psi-\chi}{\varrho}\right)\right), \tag{49}$$

and

$$\psi_l = \frac{\chi}{\rho}. \tag{50}$$

At the poles $\psi_l = \sin\psi/\rho$. The system of Eqs. (41) and (46)–(50) is solved numerically. The integration over the arc length l is performed from both poles so that the relative area of the calculated shape is equal to 1. Then, the validity of the constraints is tested and new initial values of the above quantities are set. The procedure is repeated until the constraints and the smoothness of the variables at

the meeting point are fulfilled up to a prescribed accuracy. The contour of the cell shape is determined using the relation

$$\frac{\mathrm{d}z}{\mathrm{d}l} = -\sin\psi. \tag{51}$$

2.5. Estimation of Constants

In order to solve the variational problem, the values of the model constants κ and ϑ should be estimated. It was previously considered[18] that the interaction constant ξ can be estimated from the bilayer bending constant. The other interaction constant ξ^* was for reasons of simplicity taken to be equal to ξ. Also here we adopt the above so that $\xi = \xi^* = k_c a_0$, where k_c is the bilayer bending constant and a_0 is the area per phospholipid molecule. The values of these quantities are taken from the literature ($k_c \simeq 20\,kT$, $a_0 = 60 \times 10^{-20}\,\mathrm{m}^2$.[30]) Further, we take it that for a giant phospholipid vesicle R_s is 10^{-5} m, corresponding to samples of vesicles obtained by electroformation.[34] It was taken that $T = 300\,\mathrm{K}$. The intrinsic curvature deviator D_m was estimated as $2 \times 10^8\,\mathrm{m}^{-1}$.[18,26] For $\tilde{k} = 0$ we thereby obtain using Eq. (37) that $\vartheta \simeq 1.5 \times 10^{-4}$, while using Eq. (34) we obtain $\kappa \simeq 7 \times 10^6$.

Being aware of diverse contributions to the direct interaction between the phospholipid molecules, we will only attempt to give a rough estimate of its order of magnitude. We estimate the energy $\tilde{k}/kT$ by the van der Waals interactions between the tails of orientationally ordered and orientationally disordered nearest neighbors of a given molecule. We take that the phospholipid molecules are distributed in a quadratic lattice and take into account the nearest tails of the neighboring molecules. The tail of a phospholipid molecule is described as a cylinder. The energy of van der Waals interaction between two cylinders with aligned geometrical axes is $w_W(\delta) = A_H L\sqrt{r_0}/24\delta^{3/2}$, where A_H is the Hamaker constant, L is the length of the cylinders, δ is the distance between the cylinders and r_0 is the radius of the cylinders. For hydrocarbons $A_H = 3\,kT/4$[35] while we take for the lipid molecules $L = 1.5\,\mathrm{nm}$, $r_0 = 3.5\,\mathrm{nm}$ and $\delta = 0.3\,\mathrm{nm}$. The estimated energy is $\tilde{k}/kT = 2w_W(\delta)/kT \simeq 1$.

3. RESULTS

If follows from Eqs. (47)–(48) that a singularity in $\mathrm{d}\chi/\mathrm{d}l$ occurs when the denominator (48) becomes equal to 0,

$$1 - \frac{2\kappa\vartheta^2}{\cosh^2(\vartheta(\frac{\sin\psi}{\rho} - \psi_l))} = 0. \tag{52}$$

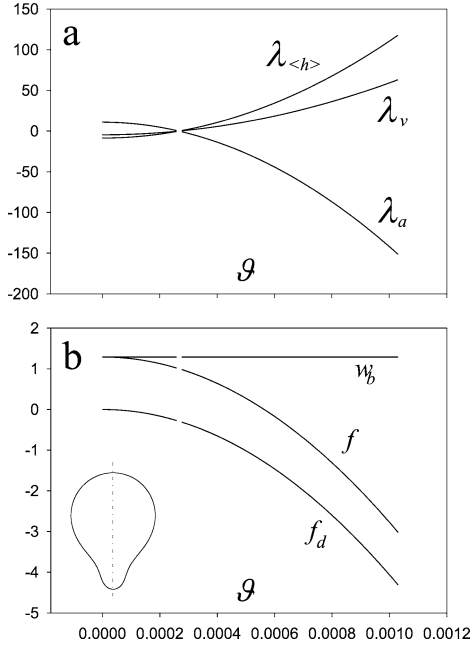

Fig. 1. a: Lagrange coefficients as a function of the interaction constant ϑ, b: bilayer membrane free energy f and the energy contributions: energy of isotropic bending w_{b}, and contribution of orientational ordering f_{d} as a function of the interaction constant ϑ; $v = 0.95$, $\langle h \rangle = 1.0422$, $\kappa = 7 \times 10^6$.

Equation (52) is fulfilled when

$$\frac{\sin\psi}{\rho} - \psi_l = \pm\frac{1}{\vartheta}\ln(\sqrt{2\kappa}\vartheta + \sqrt{2\kappa\vartheta^2 - 1}), \tag{53}$$

i.e. when the curvature deviator attains a certain constant value determined by the constants κ and ϑ. For almost globular shapes (shapes that exhibit small principal curvatures over all their area) the argument of the cosh is almost zero so that $\cosh \simeq 1$. For such shapes there would be a relatively narrow interval of chosen constants κ and ϑ, $(2\kappa\vartheta^2 \simeq 1)$ for which the singularity could occur. Fig. 1 shows how the global Lagrange multipliers of an almost globular shape with chosen relative volume and average mean curvature and a chosen constant κ change upon increase of the constant ϑ. It could be expected that the singularity would eventually be reached for high enough values of ϑ. We call the shape where the singularity first occurs the critical shape. We were able to overcome the interval of ϑ corresponding to shapes with at least one singularity by extrapolating the solution (the Lagrange multipliers and the boundary conditions) over this narrow interval. Within this interval we could not solve the variational problem numerically. This

is indicated by the gap in the curves (Figs. 1a,b). It can also be seen in Fig. 1a that all the Lagrange multipliers approach zero within this interval.

Figure. 1b shows the corresponding dependence of the energy contributions on the value of the constant ϑ. The isotropic bending energy w_b, the deviatoric energy f_d and the sum of these two terms $f = w_b + f_d$ are depicted. It can be seen that close to the interval where the singularity occurs and the Lagrange multipliers approach zero, the dependence of the energy on ϑ indicates no discontinuity. When the interaction constant ϑ is increased over the entire range where the shapes could be calculated (Fig. 1) the shape change is so minute that the shape appears the same (see inset).

Increasing the constant ϑ in a shape that attains many different values of c_1 and c_2 along the contour (such as the pear-shape with a narrow neck) would first yield a singularity (reach the critical shape) at a single point on the contour (on a ring of axisymmetric shape) in the neck region. It is of interest to study the behavior of the solutions of the variational problem close to the critical shape. Starting with the constants κ and ϑ that are high enough to yield a solution above the interval where the singularity occurs in at least one point on the contour, we approached the critical shape with a somewhat narrower neck by decreasing the constant κ.

Figure 2 shows the contour of the shape and the corresponding fraction of the molecules in the lower energy state, i.e. the ordering of the phospholipid molecules; gray lines correspond to the shape that is more remote to the critical ϑ while black lines correspond to the shape that is closer to the critical ϑ. It can be seen in both cases that the fraction of the molecules in the lower energy state increases in the neck region. In the neck the curvature deviator is higher and the orientational ordering becomes more pronounced. As the critical ϑ is approached, the maximum of the orientational distribution function becomes narrower and the peak becomes sharper. The neck of the pear-shape becomes shorter and exhibits a more abrupt width change for the shape that is closer to the critical ϑ.

Figure 3 shows the numerator (Eq. (49)), the denominator (Eq. (48)) and the derivative $\mathrm{d}\chi/\mathrm{d}l = \mathcal{A}/\mathcal{B}$ along the contour as a function of the symmetry axis of the shapes depicted in Fig. 2. In the shape that is closer to the critical shape (case b) the denominator attains lower absolute values along the whole contour while it approaches 0 at a certain point in the neck region. Correspondingly, the derivative $\mathrm{d}\chi/\mathrm{d}l$ reaches higher values and changes abruptly in the vicinity of this point forming sharp peaks. In the shape that is more remote to the critical shape (case a), the absolute values of the denominator and of the numerator are higher, while the values of the derivative $\mathrm{d}\chi/\mathrm{d}l$ are lower. The peaks formed by the derivative $\mathrm{d}\chi/\mathrm{d}l$ are milder. The arc length where the derivative $\mathrm{d}\chi/\mathrm{d}l$ strongly changes diminishes as the critical shape is approached.

We studied the formation of narrow neck(s) i.e. the sequence of shapes of increasing average mean curvature.[36] Figure 4 shows how the free energy of

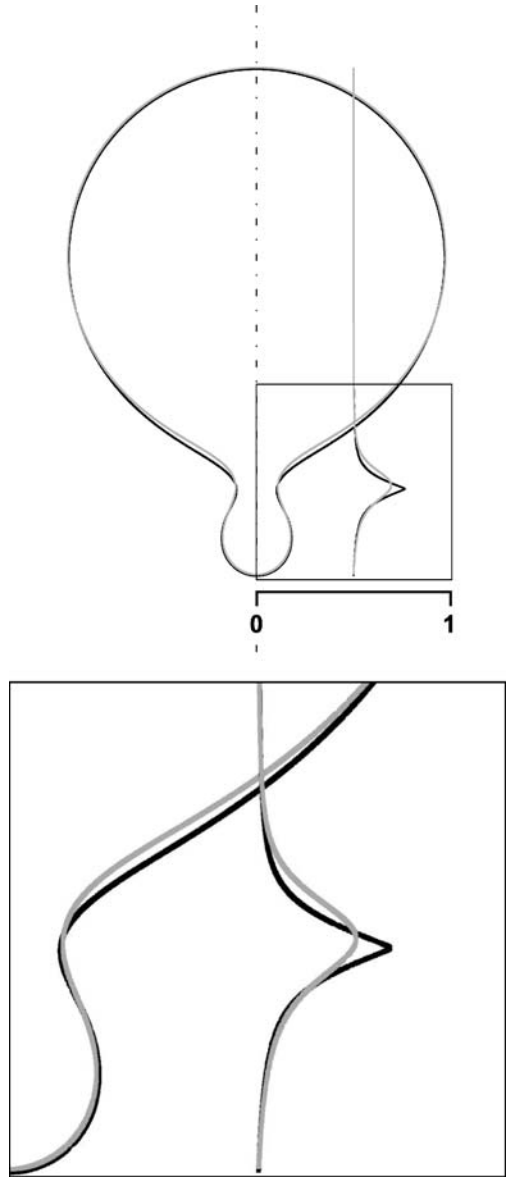

Fig. 2. Two shapes illustrating the approach to the critical shape with singularity in the Euler–Lagrange differential equation and the corresponding orientational distribution functions. The shape that is closer to the critical shape ($\kappa = 1735.5$, black) has a shorter neck and a sharper distribution peak than the shape that is more remote from the critical shape ($\kappa = 2800$, gray). For both shapes $v = 0.95$, $\vartheta = 0.02456$, $\langle h \rangle = 1.11543$.

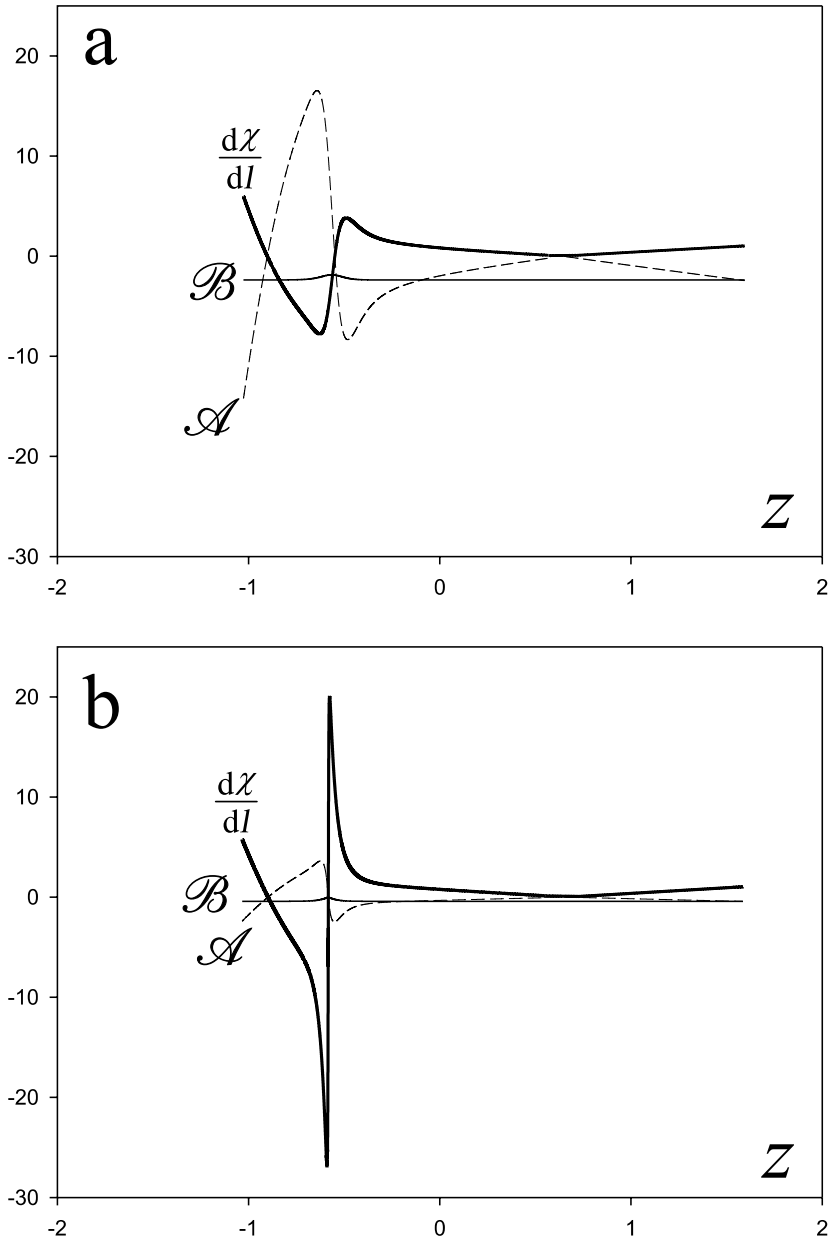

Fig. 3. Approach to the critical shape with singularity in the Euler differential equation. The numerator $\mathcal{A}$, the denominator $\mathcal{B}$ and the derivative $d\chi/dl$ are shown for both shapes (a and b, respectively) presented in Fig. 2.

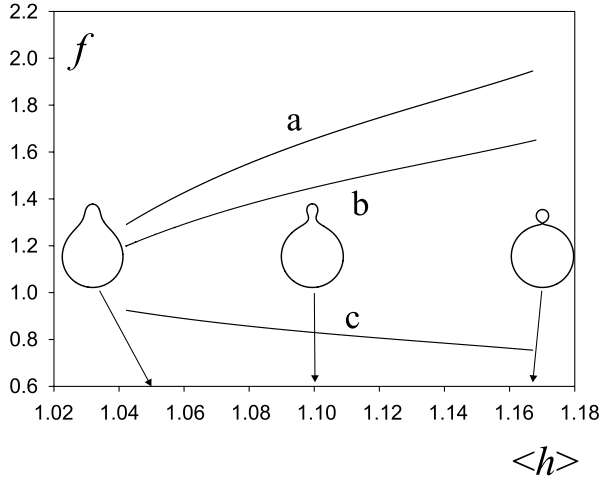

Fig. 4. Bilayer membrane free energy as a function of the average mean curvature of the vesicle with $v = 0.95$; a: isotropic bending, b: orientational ordering of independent molecules $\vartheta = 1.5 \times 10^{-4}$, $\kappa = 7 \times 10^6$, c: orientational ordering of interacting molecules $\vartheta = 3 \times 10^{-4}$, $\kappa = 7 \times 10^6$.

the vesicle changes upon increase of the average mean curvature for a vesicle of a given relative volume $v = 0.95$ and size $R_s = 10^{-5}$ m. Case a corresponds to isotropic bending only, case b corresponds to the quadrupolar ordering of independent molecules ($\tilde{k}/kT = 0$), while case c also considers direct interactions between phospholipid molecules ($\tilde{k}/kT = 1$). The energy of isotropic bending w_b increases along the sequence[38] while the energy of deviatoric bending f_d decreases along the sequence. The behavior of the sum of the two contributions exhibits the difference in the relative rate of change of the two contributions. In the case b (if the molecules are considered as independent) the decrease of the energy of the deviatoric bending is not strong enough to overcome the increase of the energy of isotropic bending w_b and f increases with increasing $\langle h \rangle$. In the case c (if direct interaction between phospholipid molecules is considered), the increase of the energy of isotropic bending w_b is overcome and the vesicle free energy decreases with increasing $\langle h \rangle$. However, for any choice of κ and ϑ, a critical shape is eventually reached at a certain $\langle h \rangle$ along the sequence. We were not able to obtain a numerical solution beyond this critical $\langle h \rangle$. For larger ϑ the critical $\langle h \rangle$ is smaller (not shown). In the results shown in Fig. 4 the critical shape was reached near the boundary of the class of pear shapes. As we could not obtain numerical solutions for $\langle h \rangle$ beyond the critical shape, we cannot say whether the limit shape composed of two spheres connected by an infinitesimal neck is eventually reached upon increase of $\langle h \rangle$.

4. DISCUSSION

In this work we studied the interdependence between quadrupolar ordering of phospholipid molecules (that are anisotropic with respect to the membrane normal) in the deviatoric curvature field and the shape of the phospholipid vesicle. The description derives from the assumption that the energy of the molecule at a given site depends on its orientation with respect to the membrane normal; the molecule spends on the average more time in the orientation that yields a lower energy according to the local deviatoric field. The model parameters are determined from the data on the intrinsic properties of the constituent molecules and their mutual interactions. A rigorous solution of the variational problem for axisymmetric shapes is sought numerically to yield the equilibrium shape and the corresponding orientational ordering distribution over the vesicle surface.

Previously, orientational ordering was described by a one-molecule partition function considering all orientations of the molecule within the plane of the membrane.[18,37,38] In this work, orientational ordering was described by a two energy state model. In using the new approach we have expressed the energy in terms of hyperbolic functions. As the hyperbolic functions are analytical, this simplified and clarified the derivation of the Euler–Lagrange equations which require analytical expression of the functional $\mathcal{L}$. More important, the two state model enabled us to introduce a simple model describing the direct interactions between phospholipid molecules.

The model describing the direct interactions between phospholipid molecules that is introduced in this work reflects close contact between the tails that is different if the molecules align in a particular way within the deviatoric field while packing to form the local curvature field. We assumed that the energy is additionally lowered if the molecules are ordered when oriented favorably, while it is increased if the molecules are ordered when oriented unfavorably. The obtained formalism renormalizes (enhances) the constant ϑ which describes the interaction of the phospholipid molecule with the deviatoric field. Therefore, the simple analytical form of the functional is also retained when the direct interactions between the molecules are taken into account. The linear approximation (Eqs. (8) and (9)) which is valid for small d_{eff} overestimates the effect of the direct interactions between phospholipid molecules for large effective deviators. In the considered sequence (Fig. 4) the shapes with a wide neck have small values of the effective deviator over the whole vesicle surface, therefore the linear approximation well represents the direct interactions between phospholipid molecules. As the slope of the $f(\langle h \rangle)$ curve is determined early in the sequence when the neck of the shape is wide, the deviation of the linear approximation from exact dependence at larger $\langle h \rangle$ does not change the conclusion that the direct interactions between phospholipid molecules promote the formation of the narrow neck. On replacing the linear approximation by a more realistic one expressing the saturation of the ordering, a

minimum in the $f(\langle h \rangle)$ curve may however be formed, corresponding to the shape with a finite narrow neck that would be energetically the most favorable.

A singularity was found in the differential equation for $\mathrm{d}\chi/\mathrm{d}l$ (Eqs. (47)–(48)). This singularity occurs at sites where the opposing effects of isotropic and deviatoric bending become equal in magnitude, i.e. where the deviatoric effects renormalize the isotropic bending to zero. A geometry is reached where the curvature is so high that the approximate model is no longer valid. Fig. 3 shows that the derivative $\mathrm{d}\chi/\mathrm{d}l$ increases when we approach the critical shape, while the numerator and the denominator both decrease over the entire shape. In the point on the contour close to the narrowest width of the neck, the denominator approaches zero. From the numerical results we could not come to a definite conclusion that the regularity condition can be imposed. We could not exclude the possibility that the derivative $\mathrm{d}\chi/\mathrm{d}l$ may in some cases increase beyond any limit. This would mean that the discontinuity in the meridian curvature that is consistent with divergence in $\mathrm{d}\chi/\mathrm{d}l$ corresponds to a finite energy. Changes of the meridian curvature over a minute arc length were recently observed in two component phospholipid vesicles with added cholesterol, where the two phospholipids were in two different liquid phases (ordered/disordered).[39] Segregation of the phospholipid was observed whereby an abrupt change in the meridian curvature could be noted in some of the two-photon micrographs. The abrupt changes in curvature appear close to the line where the two phases are in contact, but rather within the disordered phase region. In some shapes the abrupt change in meridian curvature appears within the disordered phase. It is argued[39] that the shape is determined by the preference of the phospholipid for a certain curvature and by the effects on the edges where the two phases meet, however the abrupt changes in the curvature within the given phase are not explained.

Experiments show that besides flat or almost flat structures, phospholipid molecules also favor other structures (hexagonal and cubic).[40–42] In hexagonal and cubic structures the principal curvatures strongly differ, so it is obvious that in these structures the molecules are sensitive to the difference between the principal curvatures. Within our description two situations are energetically favorable: the state $H = D = 0$ (flat membrane) where both the energy of isotropic bending and the deviatoric energy are zero, or the state $H \neq 0$, $D \neq 0$, where the deviatoric energy contribution is large and negative so that it counterbalances the positive energy contribution of isotropic bending.

As the model of quadrupolar ordering successfully described shapes with connected nanotubes in one-component phospholipid bilayer membranes,[18] we suspected that it might prove successful also in explaining the stability of the narrow neck in such systems. We found our expectations to be correct, as the free energy of the vesicle decreases with narrowing of the neck of the vesicle.

This result reveals a possible role of quadrupolar ordering in phospholipid bilayer systems that is more general than initially expected. In previous works

involving inclusions, most of the effect was found to derive from strongly anisotropically curved regions with accumulated inclusions.[21–27, 38] Similarly, in describing the stability of nanotubular protrusions in a one-component phospholipid membrane [18] where we used a parametric model composed of a sphere (where the deviatoric field is zero and there is no ordering) and a protrusion (where the deviatoric field is high), the effect came from quadrupolar ordering of phospholipid molecules on the nanotubular protrusion. The rigorous solution of the variational problem (Fig. 4) shows that the effect of quadrupolar ordering on the free energy of the vesicle is also important in shapes where there are no regions of very high curvature deviator. Except for in the vicinity of the singularity, the local ordering is low over most of the membrane area, while the equilibrium shape could hardly be distinguished from the corresponding shape calculated by minimization of the Helfrich local bending energy. However, as the values of the free energy are considerably affected, the quadrupolar ordering of phospholipid molecules provides a particular interpretation of the trajectories representing the observed processes within the phase diagram of possible shapes.

A possible explanation for the stability of the narrow neck was proposed by the area-difference-elasticity model.[9] The ADE model[8–9] is based on the minimization of the Helfrich local energy of isotropic bending while another important energy contribution comes from a nonlocal term - the relative stretching of the two membrane layers. The nonlocal bending energy is given by two parameters, the nonlocal bending constant $\bar{\kappa}$ and the relaxed area difference between the two membrane monolayers ΔA_0. The set of possible shapes obtained by the numerical solution of the relevant system of Euler-Lagrange differential equations is identical to the set obtained by the minimization of the local bending energy,[9] but by considering the nonlocal bending energy, for chosen data, the shape of the lowest total energy may differ from the shape with the lowest energy of local bending. In the sequence of shapes starting from a pear shape and leading to two spheres connected by an infinitesimal neck, the energy of isotropic bending monotonously increases with $\langle h \rangle$, while adding the nonlocal bending energy consisting of the quadratic function of $\langle h \rangle$ may, for appropriate choice of the relaxed area difference between the two monolayers ΔA_0, result in a decrease of the free energy towards the limit shape. The limit shape therefore becomes the shape of minimal free energy which is interpreted as the stability of the infinitesimal neck. Within the area-difference-elasticity model, a certain threshold value of ΔA_0 is therefore necessary to obtain a stable neck, assigned by a line $\mathrm{L}^{\mathrm{pear}}$ within the $(v, \Delta A_0/(2\delta R_\mathrm{s}))$ phase diagram,[9] where δ is the distance between the two monolayer neutral surfaces. If we take the experimentally determined value of $\alpha = \bar{\kappa}/\pi k_\mathrm{c} \simeq 0.64$,[8.5,9] we get for $v = 0.95$ the threshold value $\Delta A_0/(2\delta R_\mathrm{s}) \simeq 3$ which yields for the membrane free energy normalized by $8\pi k_\mathrm{c}$ (equivalent to the relative free energy depicted in Fig. 4), $f \in [8.5, 9]$ for the range of $\langle h \rangle$ corresponding to Fig. 4. For a vesicle with the narrow neck (at the end of the sequence), about one fourth of the

whole free energy comes from the local bending term and the rest from the relative stretching term. The relatively high energy of relative stretching implies that the tension within the membrane is high. It could be argued that the membrane would tend to relax, for example by a tension - induced transport of molecules between the layers through transient pores.[44] By considering the mechanism proposed in this work the formation of the neck is energetically favorable for any initiation mechanism. The membrane free energy decreases as the region of increasing curvature deviator increases while the free energy values remain within the same range (Fig. 4). Similar to exovesiculation (Fig. 4), an energy decrease could also be expected for endovesiculation, by using the same values of the model constants (ϑ and κ). The deviatoric effects could not determine the general direction of the shape change of the globular vesicle, but once the neck(s) start(s) to form, the deviatoric effects will provide a mechanism for its stabilization.

The formation of a stable neck needs to be further clarified. The mechanism of quadrupolar ordering is complementary to the mechanisms of local and nonlocal isotropic elasticity of the ADE model. Both mechanisms can be considered in describing the stable neck. The quadrupolar ordering decreases the free energy, therefore a lower value of $\Delta A_0/(2\delta R_s)$ is needed to obtain a minimum of free energy at the average mean curvature corresponding to the vesicle with a narrow neck. Taking both mechanisms into account, for $\vartheta = 1.5 \times 10^{-4}$, $\kappa = 7 \times 10^6$ and $\alpha = 0.64$ we obtain a shallow minimum of free energy close to the limit shape at $\langle h \rangle = 1.16$ for $\Delta A_0/(2\delta R_s) = 1.9$ (instead of $\simeq 2.4$ as estimated by the ADE model alone). Consequently, throughout the sequence, the free energy and the corresponding energy of relative stretching are considerably lowered ($\simeq 2.7$) with respect to the ADE model alone ($\simeq 5$). The two mechanisms support each other in promoting the formation of the neck and in its stabilization.

The proposed hypothesis of quadrupolar ordering of phospholipid molecules in a deviatoric field can describe the stability of shapes with strongly anisotropically curved structures in heterogeneous membranes,[21–27),(38] in inorganic micro and nanostructures[28] and in one-component phospholipid vesicles.[18] An explanation of the above features could not be provided by the mechanism of isotropic elasticity (a more extensive discussion on this issue can be found in[18,21,25,45]). In this work we further support the hypothesis of quadrupolar ordering of phospholipid molecules in a deviatoric field by showing that the quadrupolar ordering of phospholipid molecules promotes the formation of a narrow neck. Also, it was shown that this effect may significantly affect the energy of phospholipid vesicles even when they are not connected to strongly anisotropically curved structures. Owing to above, we suggest that quadrupolar ordering in a deviatoric field should be considered as a possible relevant mechanism that complements the description of bilayered vesicular structures.

A description of the phospholipid membrane by deviatoric elasticity that was inspired by the problem of the stable neck was previously proposed by

Fischer.[46,47] The deviatoric effect was characterized by a constant called the spontaneous warp. However, the value of the spontaneous warp was then considered to be zero by the argument that the phospholipid membrane as observed in experiments is locally flat. Nanostructures of phospholipid membrane that were detected experimentally[13,15] prove that the phospholipid membrane is not always locally flat. We elaborated the problem of deviatoric elasticity by deriving the deviatoric properties of the phospholipid membrane from the microscopic picture. Our work therefore supports the ideas proposed by Fischer. [46,47]

Also, evidence was presented[48] that the neck may elongate. This indicates that in the sequence starting with a pear shape and promoting a neck, the formation of the limit shape composed of two spheres connected by an infinitesimal neck would not be reached. To further explore such a process, more insight into the solution of the variational problem beyond the singularities and a deeper understanding of the behavior of the system on the molecular level would be required.

APPENDIX

In the Appendix we present a generalized form of the Euler-Lagrange differential equations for axisymmetric shapes, where the functional $\mathcal{L}$ is given as a function of the mean curvature h and the difference $d = \mid c_1 - c_2 \mid /2$,

$$\mathcal{L} = \mathcal{F}(h)\rho + \mathcal{G}(d)\rho + \lambda_a \frac{\rho}{2} + \lambda_v \frac{3}{4}\rho^2 \sin\psi + \frac{\rho}{2}\lambda_{\langle h\rangle} h + \lambda(\rho_l - \cos\psi), \quad \text{(A.1)}$$

By considering that

$$\frac{\partial \mathcal{L}}{\partial \rho} = \left(\frac{\partial \mathcal{F}}{\partial \rho} + \frac{\partial \mathcal{G}}{\partial \rho}\right)\rho + \mathcal{F}(h) + \mathcal{G}(d) + \frac{3}{2}\lambda_v \rho \sin\psi + \lambda_a \frac{1}{2} + \frac{1}{2}\lambda_{\langle h\rangle}\left(\frac{\partial h}{\partial \rho}\rho + h\right), \quad \text{(A.2)}$$

$$\frac{\partial \mathcal{L}}{\partial \psi} = \left(\frac{\partial \mathcal{F}}{\partial \psi} + \frac{\partial \mathcal{G}}{\partial \psi}\right)\rho + \frac{3}{4}\lambda_v \rho^2 \cos\psi + \frac{1}{2}\lambda_{\langle h\rangle}\frac{\partial h}{\partial \psi}\rho + \lambda \sin\psi), \quad \text{(A.3)}$$

$$\frac{\partial \mathcal{L}}{\partial \psi_l} = \frac{1}{2}\left(\frac{\partial \mathcal{F}}{\partial h} - \frac{\partial \mathcal{G}}{\partial d}\right)\rho + \frac{1}{4}\lambda_{\langle h\rangle}\rho, \quad \text{(A.4)}$$

$$\frac{\mathrm{d}}{\mathrm{d}l}\frac{\partial \mathcal{L}}{\partial \psi_l} = \frac{1}{2}\cos\psi\left(\frac{\partial \mathcal{F}}{\partial h} - \frac{\partial \mathcal{G}}{\partial d}\right) + \frac{1}{2}\rho\left(\frac{\mathrm{d}}{\mathrm{d}l}\frac{\partial \mathcal{F}}{\partial h} - \frac{\mathrm{d}}{\mathrm{d}l}\frac{\partial \mathcal{G}}{\partial d}\right) + \frac{1}{4}\lambda_{\langle h\rangle}\cos\psi, \quad \text{(A.5)}$$

$$\frac{\partial \mathcal{F}}{\partial \rho} = \frac{\partial \mathcal{F}}{\partial h}\frac{\partial h}{\partial \rho},\ \frac{\partial \mathcal{G}}{\partial \psi} = \frac{\partial \mathcal{G}}{\partial d}\frac{\partial d}{\partial \psi},\ \frac{\partial \mathcal{F}}{\partial \psi} = \frac{\partial \mathcal{F}}{\partial h}\frac{\partial h}{\partial \psi},\ \frac{\partial \mathcal{G}}{\partial \rho} = \frac{\partial \mathcal{G}}{\partial d}\frac{\partial d}{\partial \rho}, \tag{A.6}$$

we obtain a system of differential equations

$$\frac{\mathrm{d}\lambda}{\mathrm{d}l} = -\frac{1}{2}\frac{\sin\psi}{\rho}\left(\frac{\partial \mathcal{F}}{\partial h} + \frac{\partial \mathcal{G}}{\partial d}\right) + \mathcal{F}(h) + \mathcal{G}(d) + \frac{3}{2}\lambda_v \rho \sin\psi + \frac{1}{2}\lambda_a + \frac{1}{4}\lambda_{\langle h\rangle}\psi_l, \tag{A.7}$$

$$\frac{\mathrm{d}}{\mathrm{d}l}\frac{\partial \mathcal{F}}{\partial h} - \frac{\mathrm{d}}{\mathrm{d}l}\frac{\partial \mathcal{G}}{\partial d} = \frac{2}{\rho}\cos\psi\frac{\partial \mathcal{G}}{\partial d} + \frac{3}{2}\lambda_v \rho\cos\psi + \frac{2}{\rho}\lambda\sin\psi. \tag{A.8}$$

In our case, where

$$\mathcal{F}(h) = \frac{1}{2}h^2, \tag{A.9}$$

$$\mathcal{G}(d) = -\frac{\kappa}{2}\ln\cosh\ 2\vartheta d. \tag{A.10}$$

we obtain the system of equations (46)–(50).

ACKNOWLEDGEMENTS

We thank V. Heinrich for the software for solving the system of Euler-Lagrange differential equations corresponding to isotropic bending. We also thank J. Guven for fruitful discussion regarding the singularity. Authors acknowledge support: S.M. from ND ERSCoR through NSF grant EPS-0132289 and from TMWFK, D.R.G. from TMWFK, A.I. from DAAD and P2-0232 and V.K.I. and B.B. from P2-0232.

REFERENCES

1. D. Nelson and T. Piran (eds.), Statistical Mechanics of Membranes and Surfaces, Jerusalem Winter School, (World Scientific, Singapore, 1989).
2. P. B. Canham, Minimum energy of bending as a possible explanation of biconcave shape of human red blood cell, *J. Theor. Biol.* **26**:61–81 (1970).
3. W. Helfrich, Elastic properties of lipid bilayers - theory and possible experiments, *Z. Naturforsch* **28c**:693–703 (1973).
4. Seifert U. Configurations of fluid membranes and vesicles, *Adv. Phys. 46*:13–137 (1997).
5. H. J. Deuling and W. Helfrich, Curvature elasticity of fluid membranes - catalog of vesicle shapes, *J. Phys. (France)* **37**:1335–1345 (1976).
6. E. Evans, Bending resistance and chemically induced moments in membrane bilayers, *Biophys. J.* **14**:923– 931 (1974).

7. W. Helfrich, Blocked lipid exchange in bilayers and its possible influence on the shape of vesicles, *Z. Naturforsch* **29c**:510–515 (1974).
8. E. A. Evans and R. Skalak, Mechanics and Thermodynamics of Biomembranes (CRC press, Boca Raton, 1980).
9. L. Miao, U. Seifert, M. Wortis and H. G. Döbereiner, Budding transitions of fluid-bilayer vesicles: effect of area difference elasticity. *Phys. Rev. E* **49**:5389–5407 (1994).
10. B. L. S. Mui, H. G. Döbereiner, T. D. Madden, and P. R. Cullis, Influence of transbilayer asymmetry on the morphology of large unilamellar vesicles, *Biophys. J.* **69**:930–941 (1995).
11. H. G. Döbereiner, O. Selchow and R. Lipowsky, Spontaneous curvature of fluid vesicles induced by trans - bilayer sugar asymmetry, *Eur. Biophys. J.* **28** 174–178 (1999).
12. H. G. Döbereiner, E. Evans, M. Kraus, U. Seifert and M. Wortis, Mapping vesicle shapes into the phase diagram: A comparison of experiment and theory, *Phys. Rev. E* **55**:4458–4474 (1997).
13. L. Mathivet, S. Cribier and P. F. Devaux, Shape change and physical properties of giant phospholipid vesicles prepared in the presence of an AC electric field, *Biophys. J.* **70**:1112–1121 (1996).
14. A. Iglič, H. Hägerstrand, M. Bobrowska-Hägerstrand, V. Arrigler, and V. Kralj-Iglič, Possible role of phospholipid nanotubes in directed transport of membrane vesicles, *Phys. Lett. A* **310**:493–497 (2003).
15. V. Kralj-Iglič, G. Gomišček, J. Majhenc, V. Arrigler, ans S. Svetina, Myelin–like protrusions of giant phospholipid vesicles prepared by electroformation, *Colloids. Surf. A* **181**:315–318 (2001).
16. M. S. Spector, A. Singh, P. B. Messersmith, and J. M. Schnur, Chiral self-assembly of nanotubules and ribbons from phospholipid mixtures, *Nanoletters* **1**:375–378 (2001).
17. A. Karlsson, R. Karlsson, M. Karlsson, A. Stromberg, F. Ryttsen and O. Orwar, Molecular engineering - networks of nanotubes and containers, *Nature* **409**:150–152 (2001).
18. V. Kralj-Iglič, A. Iglič, G. Gomišček, F. Sevšek, V. Arrigler and H. Hägerstrand, Microtubes and nanotubes of a phospholipid bilayer membrane, *J. Phys. A: Math. Gen.* **35**:1533–1549 (2002).
19. D. C. Chang, B. M. Chassy, J. A. Saunders and A. E. Sower eds., Guide to electroporation and electrofusion, (Academic Press, New York, 1992).
20. E. Neumann, A. E. Sowers and C. A. Jordan eds., Electroporation and electrofusion in cell biology, (Plenum Press, New York and London, 1989).
21. V. Kralj-Iglič, A. Iglič, H. Hägerstrand and P. Peterlin, Stable tubular microexovesicles of the erythrocyte membrane induced by dimeric amphiphiles, *Phys. Rev. E* **61**:4230–4234 (2000).
22. M. Bobrowska-Hägerstrand, V. Kralj-Iglič, A. Iglič, K. Bialkowska, B. Isomaa and H. Hägerstrand, Torocyte membrane endovesicles induced by octaethyleneglycol dodecylether in human erythrocytes, *Biophys. J.* **77**:3356–3362 (1999).
23. H. Hägerstrand, V. Kralj–Iglič, M. Fošnarič, M. Bobrowska–Hägerstrand, A. Wrobel, L. Mrowczynska, T. Söderström and A. Iglič, Endovesicle formation and membrane perturbation induced by polyoxyethileneglycolalkylethers in human erythrocytes, *Biochim. Biophys. Acta* **1665**:191–200 (2004).
24. M. Kandušer, M. Fošnarič, M. Šentjurc, V. Kralj-Iglič, H. Hägerstrand, A. Iglič and D. Miklavčič, Effect of surfactant polyoxyethylene glycol (C12E8) on electroporation of cell line DC3F, *Colloids Surf. A* **214**:205–217 (2003).
25. A. Iglič and V. Kralj-Iglič, Effect of anisotropic properties of membrane constituents on stable shape of membrane bilayer structure, in: H. Ti Tien, A. Ottova-Leitmannova, eds., Planar Lipid Bilayers (BLMs) and Their Applications, (Elsevier, Amsterdam, London, 2003).
26. M. Fošnarič, V. Kralj-Iglič, K. Bohinc, A. Iglič and S. May, Stabilization of pores in lipid bilayers by anisotropic inclusions, *J. Phys. Chem.* **107**:12519–12526 (2003).
27. A. Iglič, M. Fošnarič, H. Hägerstrand and V. Kralj-Iglič, Coupling between vesicle shape and the non-homogeneous lateral distribution of membrane constituents in Golgi bodies, *FEBS Lett.* **574**:9–12 (2004).

28. V. Kralj-Iglič, M. Remškar, G. Vidmar, M. Fošnarič and A. Iglič, Deviatoric elasticity as a possible physical mechanism explaining collapse of inorganic micro and nanotubes, *Phys. Lett.* **296**:151–155 (2002).
29. J. F. Nagle, Theory of the main lipid bilayer phase transition, *Annu. Rev. Phys. Chem.* **3**:157–195 (1980).
30. G. Cevc and D. Marsh, Phospholipid bilayers, (Wiley–Interscience, New York, 1987).
31. U. Seifert, J. Shillcock and P. Nelson, Role of bilayer tilt difference in equilibrium membrane shapes, *Phys. Rev. Lett.* **77**:5237–5240 (1997).
32. H. Nagano, T. Nakanishi, H. Yao and K. Ema, Effect of vesicle size on the heat capacity anomaly at the gel to liquid- crystalline phase transition in unilamellar vesicles of dimiristoylphosphatidylcholine, *Phys. Rev. E* **52**:4244–4250 (1995).
33. T. L. Hill, An Introduction to statistical Thermodynamics, (General Publishing Company, Toronto) pp. 209–211(1986).
34. M. I. Angelova, S. Soleau, Ph. Meleard, J. F. Faucon and P. Bothorel, Preparation of giant vesicles by external AC electric field: kinetics and application, *Prog. Colloid Polym. Sci.* **89**:127–131 (1992).
35. J. Israelaschvili, Intermolecular and Surface Forces, (Academic Press, London, 1992).
36. R. Lipowsky, The conformation of membranes, *Nature* **349**:475–481 (1991).
37. J. B. Fournier, Nontopological saddle splay and curvature instabilities from anisotropic membrane constituents, *Phys. Rev. Lett.* **76**:4436–4439 (1996).
38. V. Kralj–Iglič, V. Heinrich, S. Svetina and B. Žekš, Free energy of closed membrane with anisotropic inclusions, *Eur. Phys. J. B* **10**:5–8 (1999).
39. T. Baumgart, S. T. Hess and W. W. Webb, Imaging coexisting fluid domains in biomembrane models coupling curvature and line tension, *Nature* **425**:821–824 (2003).
40. B. deKruijff, Lipids beyond the bilayer, *Nature* **386**:129–130 (1997).
41. S. S. Funari and G. Rapp, A continuous topological change during phase transitions in amphiphile - water systems, *Proc. Natl. Acad. Sci. U.S.A.* **96**:7756–7759 (1999).
42. M. Rappolt, A. Hickel, F. Bringezu and K. Lohner, Mechanism of the lamellar/inverse hexagonal phase transition examined by high resolution x-ray diffraction, *Biophys. J.* **84**:3111–3222 (2003).
43. W. C. Hwang and R. A. Waugh, Energy of dissociation of lipid bilayer from the membrane skeleton of red blood cells, *Biophys. J.* **72**:2669–2678 (1997).
44. R. M. Raphael and R. E. Waugh, Accelerated interleaflet transport of phosphatidylcholine molecules in membranes under deformation, *Biophys. J.* **71**:1374–1388 (1996).
45. B. Babnik, D. Miklavčič, M. Kandušer, H. Hägerstrand, V. Kralj–Iglič and A. Iglič, Shape transformation and burst of giant POPC unilamellar liposomes modulated by nonionic detergent C12E8, *Chem. Phys. Lipids* **125**:123–138 (2003).
46. T. Fischer, Bending stiffness of lipid bilayers. II. Spontaneous curvature of the monolayers. *J. Phys. II (France)* **2**:327–336 (1992).
47. T. Fischer, Bending stiffness of lipid bilayers. III. Gaussian curvature, *J. Phys. II (France)* **3**:337–343 (1993).
48. T. Fischer, Mechanisms for determining the time scales in vesicle budding, *Phys. Rev. E* **50**:4156–4166 (1994).